INVESTIGATION OF HYDRODYNAMICS OF ALUMINA OXIDE MELT IN A COLD CRUCIBLE AT CONTINUOUS MELTING AND DISCHARGING

KICHIGIN[1] V., GEZA[1] V., NACKE[1] B., POZNIAK[2] I.
[1] Institute of Electrotechnology, Leibniz University Hannover,
Wilhelm-Busch-Str. 4, 30167 Hannover
[2]St. Petersburg State Electrotechnical University, Prof. Popov str., 5, 197376,
St. Petersburg, Russia
E-mail: olin24@yandex.ru

Abstract: A distinctive feature of induction furnaces with cold crucible is skull melting without introduction any impurities in the melt and overheating of the melt over 3000°C at air. Therefore the technology of induction melting in cold crucible is suitable for high temperature synthesis of oxide materials. However, the dispersion of synthesized oxide material as monolithic ingot is not always technically advantageous. Therefore, the paper proposes a new technology for continuous melting and pouring of oxide melts. In the article the results of hydrodynamics of the melt flow and the temperature field during pouring on the basis of numerical simulation with taking into account the forced and free convection are presented. Beside the melt flow inside the cold crucible special attention is paid also to the behavior of the pouring stream. The numerical results are compared with experimental data of melting and pouring experiments in the skull melting installation at the Institute of Electrotechnology in Hannover.

1. Introduction

The offer technology of continuous pouring of the oxide melt is using method of the induction melting in the cold crucible [1]. For stability condition of continuous pouring of the melt it is necessary to support required temperatures near pouring hole and on the surface of the melt. The required temperature of the melt surface provides the specified productivity of the raw melting. Technological parameters of the system are configured such a way that pouring rate of the melt and melting rate of the raw are the same. The melting process and pouring occurs in a continuous quasi- stationary mode. Maintaining equal productivities of the melting raw and pouring directly depends on the stabilization of the temperature field in the melt. On the other hand, in the temperature field influence non-stationary hydrodynamic flows in the melt, temperature dependences of the physical properties of the melt, formation the skull and crusts in the pouring hole region, occurrence of oscillations of the melt surface uneven loading raw. Therefore, for the system parameters optimization necessary to define boundaries zone of the insensitivity temperature field in the melt, depending on the above disturbing factors. Thereby, for the investigation can be selected the next tasks:

- optimization geometry of the pouring hole,
- appearing of skull layer on the pouring hole,
- instability of the melt stream.

Induction system for the continuous pouring is shown on the Figure 1, it consist from inductor, crucible, bottom and separator which are cooled down by water. The separator is installed between the pouring region and the main surface of the melt, and prevents the raw in the pouring hole.

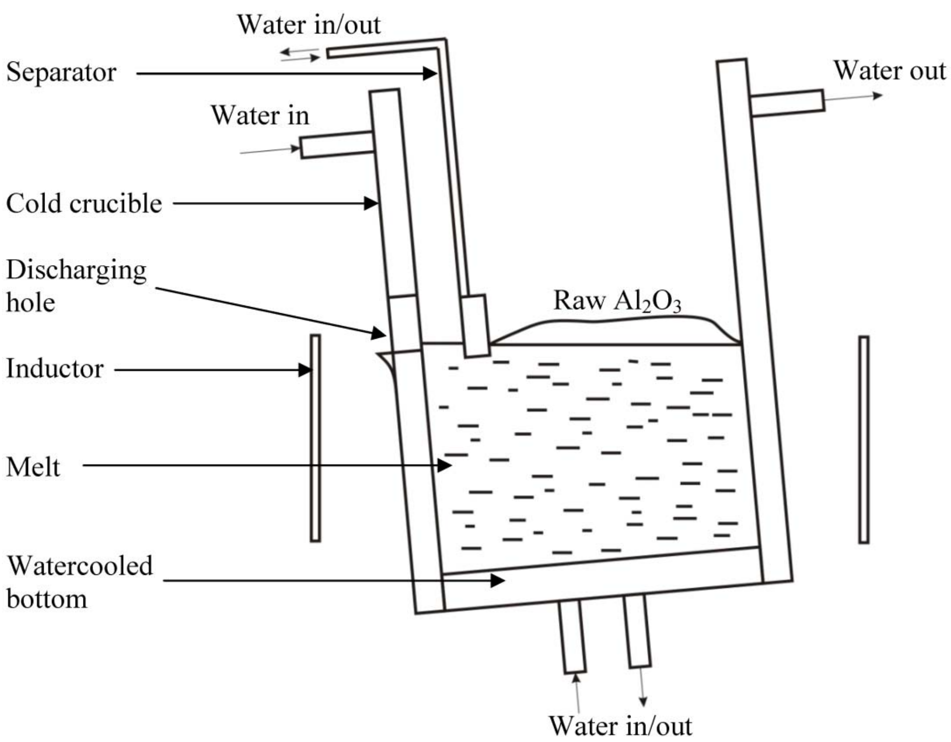

Figure 1: Induction furnace for continuous melting and discharging of oxide melt.

To prevent melt dripping on the wall of the crucible in the construction of the pouring hole nozzle is provided and also crucible is tilted to the horizon.

2. Mathematical model

Calculation of electromagnetic (EM) problem is performed using ANSYS software [2]. The obtained solution data (EM forces, Joule heat sources) are imported in fluid dynamic calculation, which is performed by CFX software [2].
The incompressible flow of melt is described by Navier-Stokes equation:

$$\frac{\partial \vec{u}}{\partial t} + \vec{u}\nabla\vec{u} = -\frac{1}{\rho}\nabla p + \nu\Delta\vec{u} + \frac{1}{\rho}\vec{f} - \beta T\vec{g}$$

Here *u* –velocity, *p* –pressure, *T* –temperature, f - Lorentz force density, β - thermal expansion coefficient, ν - kinematic viscosity.
Thermal processes in melt are described by heat transfer equation:

$$\frac{\partial T}{\partial t} + \vec{u}\nabla T = \frac{\lambda}{c\rho}\Delta T + q$$

Here λ - thermal conductivity, c - specific heat, q - Joule heat density. Constant temperature $T=T_{melt}$ boundary condition was used walls and bottom with no slip for flow field, which corresponds to solid-liquid interface between melt and skull (Figure 2). Top surface is treated differently in both sections. In the main part inflow with fixed temperature and flow rate Q is used - this condition represents continuous charge of new material. This condition is however idealized, because in experiment charging is not constant over whole area. In the smaller area, which is isolated by separator, radiation boundary condition with free slip is used.

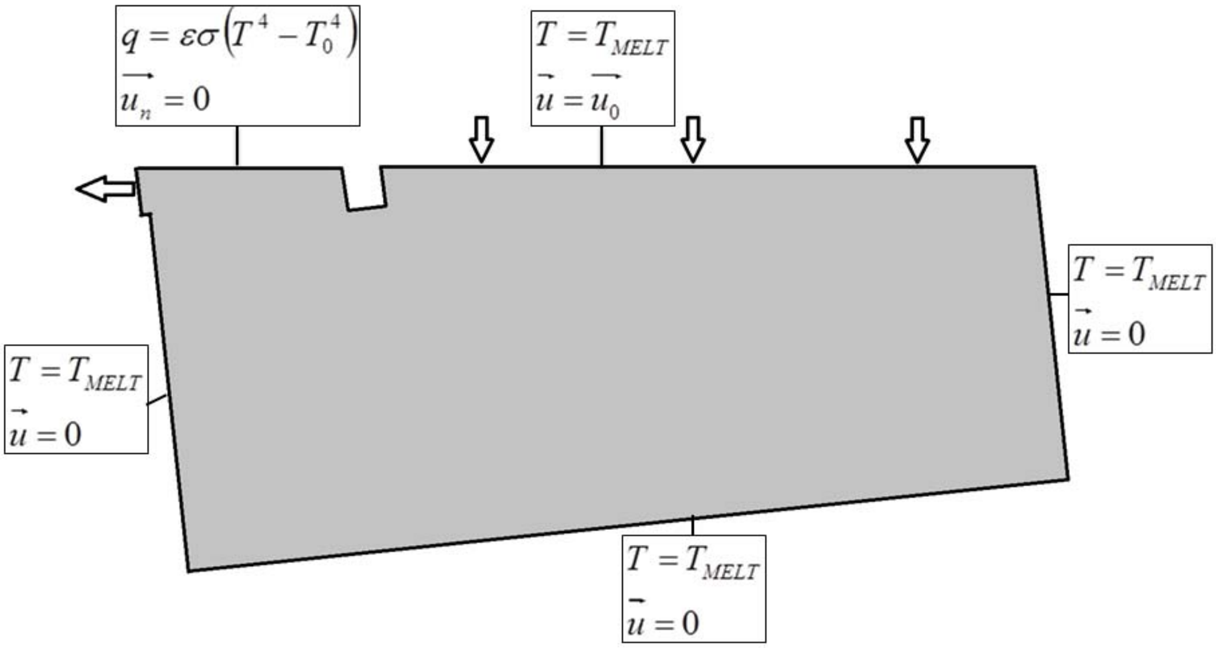

Figure 2: Calculation area and boundary conditions for hydrodynamic and thermal problem.

As in all problems with oxide melts, material properties are strictly temperature dependent [3, 4]. However, aluminum oxide data for high temperatures are limited and therefore electromagnetic conductivity temperature dependence was neglected, and decoupled problem is solved (EM sources calculated once and imported in fluid dynamic simulations). Thermal expansion coefficient is also known only for solid state of aluminum oxide and therefore influence of this value was also investigated.

3. Results

Simulations are performed for different charging rates on top surface (0.2 kg/min - 1.2 kg/min). Same flow and temperature field character is observed for all cases, certain differences are observed only in peak values. Figure 3 shows temperature distribution in vertical cross section of crucible, which also matches to symmetry plane. It is visible that in middle part of the crucible temperature iso-lines are horizontal and no vertical motion due to buoyancy forces can appear in this part. In the left bottom corner of this figure it is visible that melt temperatures here are significantly lower than in other regions of crucible. On the right side of Figure 3 near wall, steep change of temperature in radial direction is observed. This region coincides with skin-layer of EM fields, where intensive Joule heating appears. Maximal temperatures are observed in the upper right corner of the crucible, which are more almost 800°C over melting temperature. The flow field is intensive only in the zone near outflow, where it reaches several centimeters per second. In the rest part of the crucible velocities are only few mm/s (Figure 4). Along whole perimeter of crucible buoyancy vertices are observed (best seen on the right side of Figure 4), which are caused by strong radial temperature gradient. These vertices are narrow in radial direction and long (length of wall) in vertical direction. In the region of outflow this vortex is more intensive and larger in radial direction. Additionally vortex is formed directly under the surface in the charge-free zone, it has velocity vectors directed downwards at the separator due to cooling of melt. Combination of these vertices and transit flow (constant flow out of the crucible) results in complicated three dimensional flow structure near the outflow. All dominant motion structures in this crucible are established by buoyancy forces and influence of Lorentz forces is small.

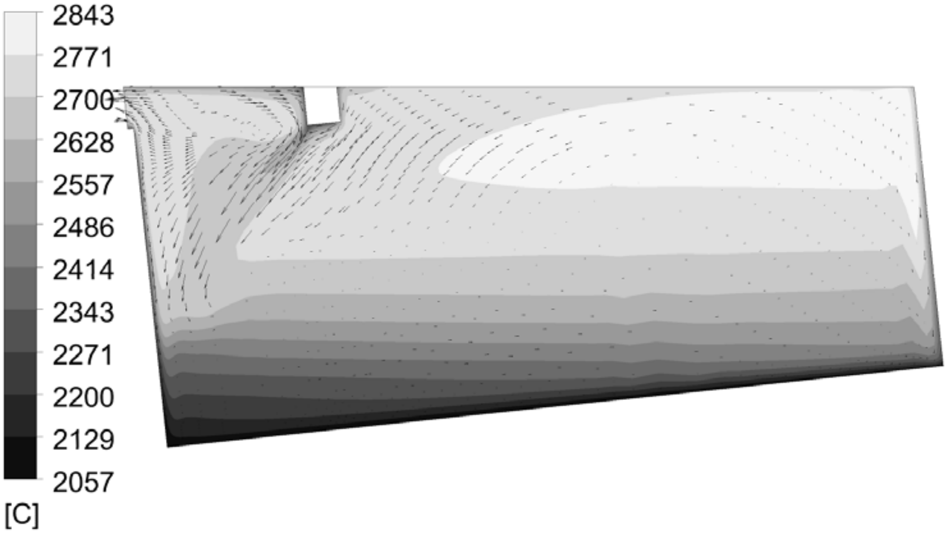

Figure 3: Distribution of temperature in vertical cross section. Arrows show velocity in this plane. Q = 800 g/min.

Figure 4: Streamlines of velocity. Q = 800 g/min.

Simulations were also performed for different flow rates and maximal and mean temperatures in the melt and at the outflow were observed. Figure 5 (left) shows this dependency. It is obvious that increased charge of cold material leads to lower melt temperatures.

Figure 5 (right) shows dependency of the melt temperatures on thermal expansion coefficient, which is not certainly known for used material. Higher thermal expansion coefficient leads to more intensive mixing and better heat fluxes through the side walls. Additionally more intensive vertical mixing leads to more heat transported through the bottom of the crucible.

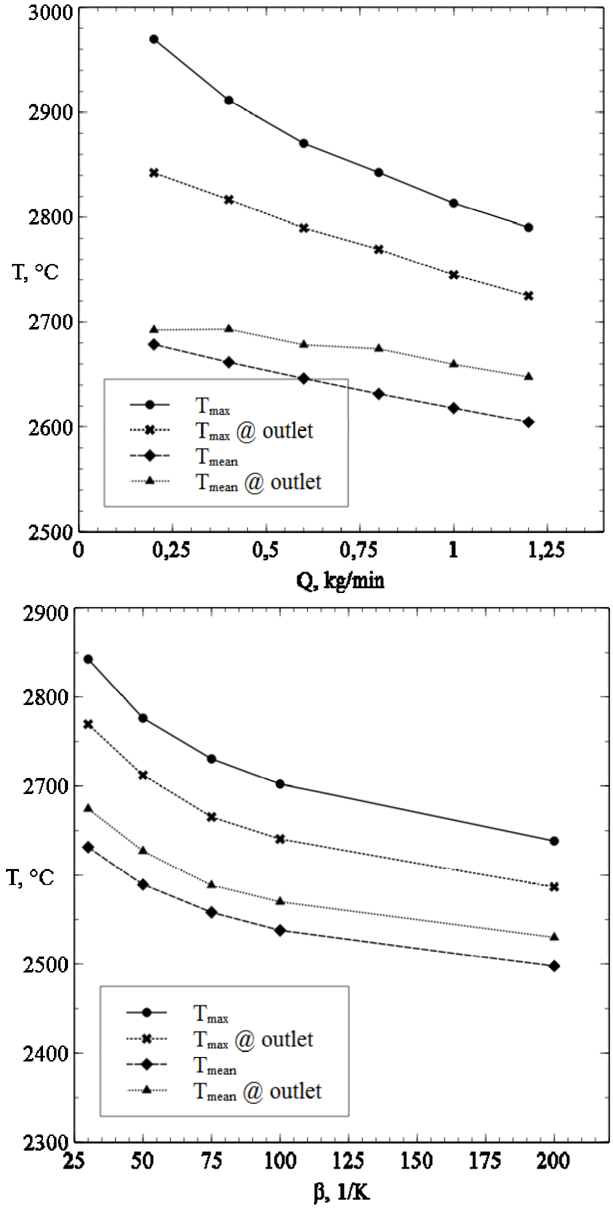

Figure 5: Dependence of temperature in melt on charge rate (left) and thermal expansion coefficient (right).

4. References

[1].Petrov, Yu.B. The Induction Melting of Oxides. Energoatomizdat, Leningrad. 1983, 104 p.
[2]. ANSYS, Inc. Theory Reference. Ansys Release 14. http://www.ansys.com
[3]. Krzyzanowski R.E., Stern Z.Yu. Thermal Properties of Non-Metallic Materials, L., "Energy", 1973.
[4]. Samsonov G.V. Physical Chemical Properties of Oxides, Publishing House "Metallurgy", 1978, 472 p.